Supplement to 'Attributing ozone and its precursors to land transport emissions in Europe and Germany'

Mariano Mertens
Institut für Physik der Atmosphäre
DLR-Oberpfaffenhofen

mariano.mertens@dlr.de

April 2020

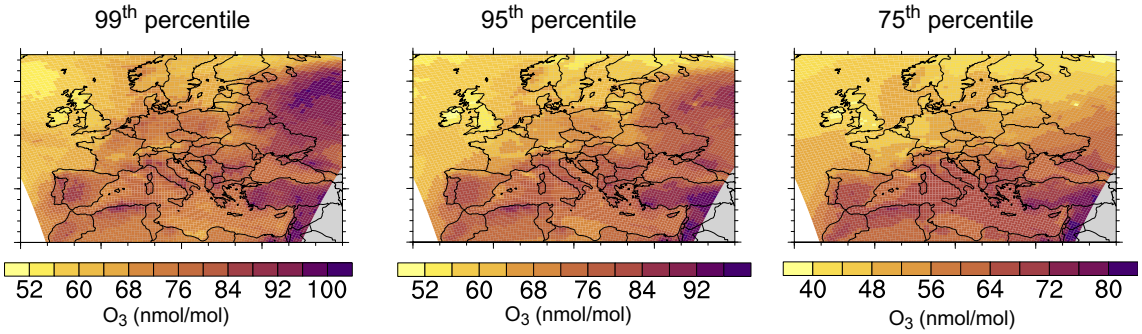

Figure S1: 99th, 95th and 75th percentile of ozone (in nmol mol^{-1}) for the period JJA 2008–2010 based on 3-hourly model output. Results of the *REF* simulation.

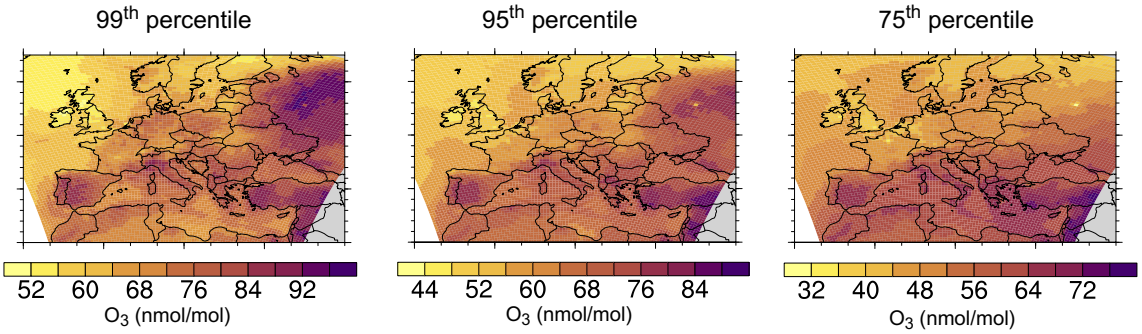

Figure S2: 99th, 95th and 75th percentile of ozone (in nmol mol^{-1}) for the period JJA 2008–2010 based on 3-hourly model output. Results of the *EVEU* simulation.

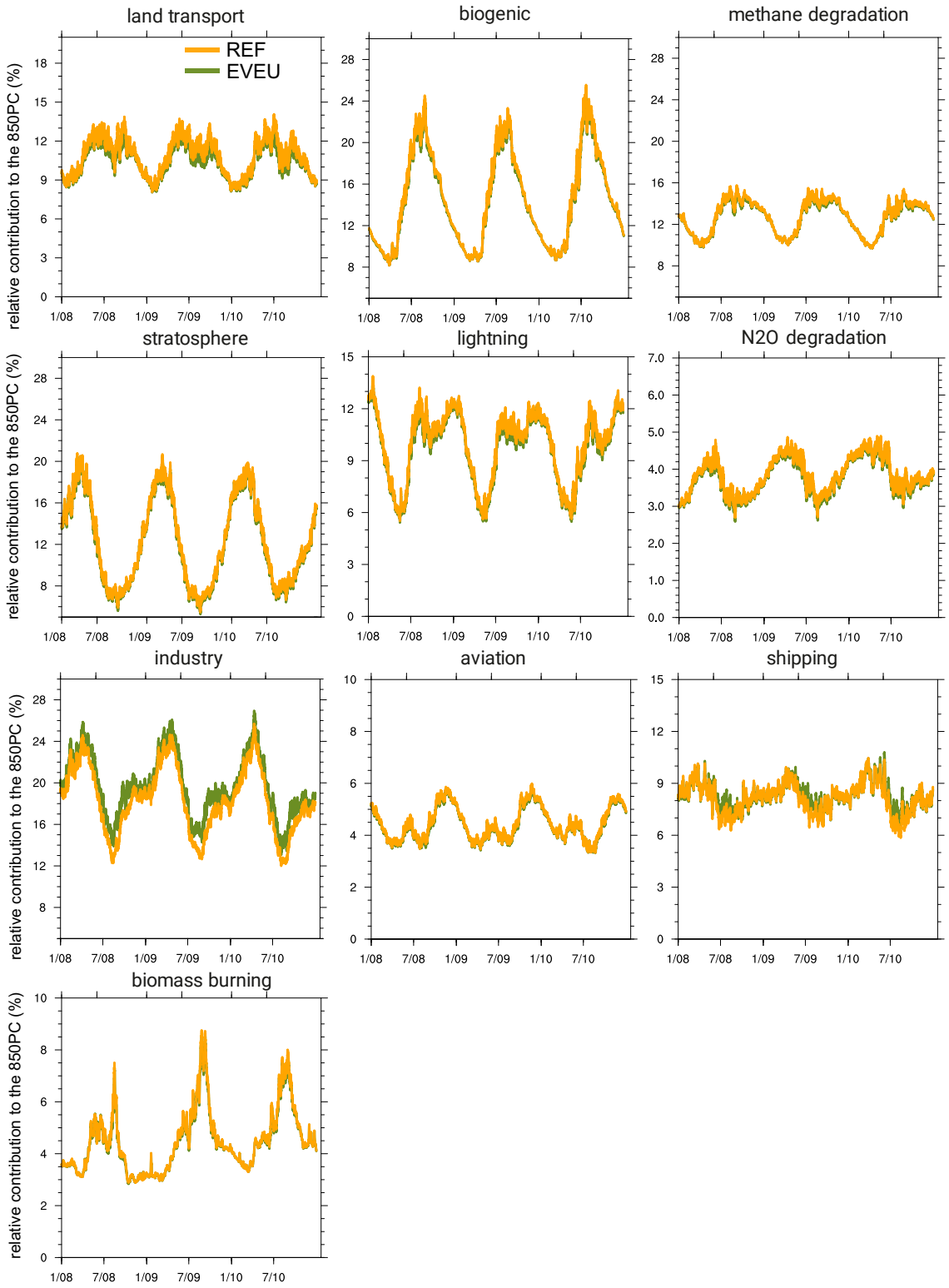

Figure S3: Relative contribution (area average for CM50 domain) of different emission sources to the ozone column up to 850 hPa.

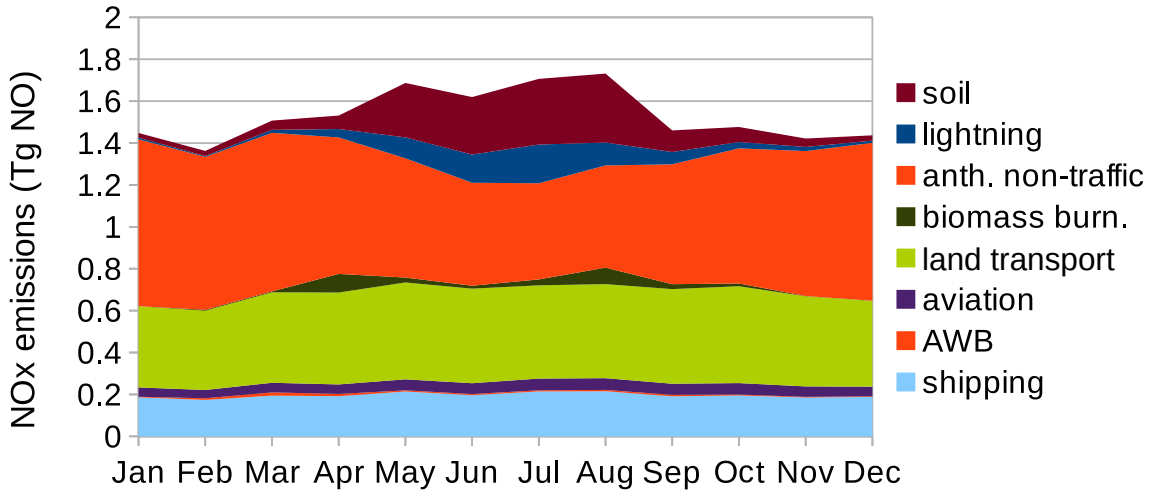

Figure S4: Monthly total emissions of NO (in Tg) for the CM50 domain for different emission sources. For the anthropogenic emissions the MAC inventory is used. Shown is the seasonal cycle for the year 2008. In different years or with the *VEU* emission inventory the seasonal cycle looks similar. Figure reproduced from Mertens (2017).

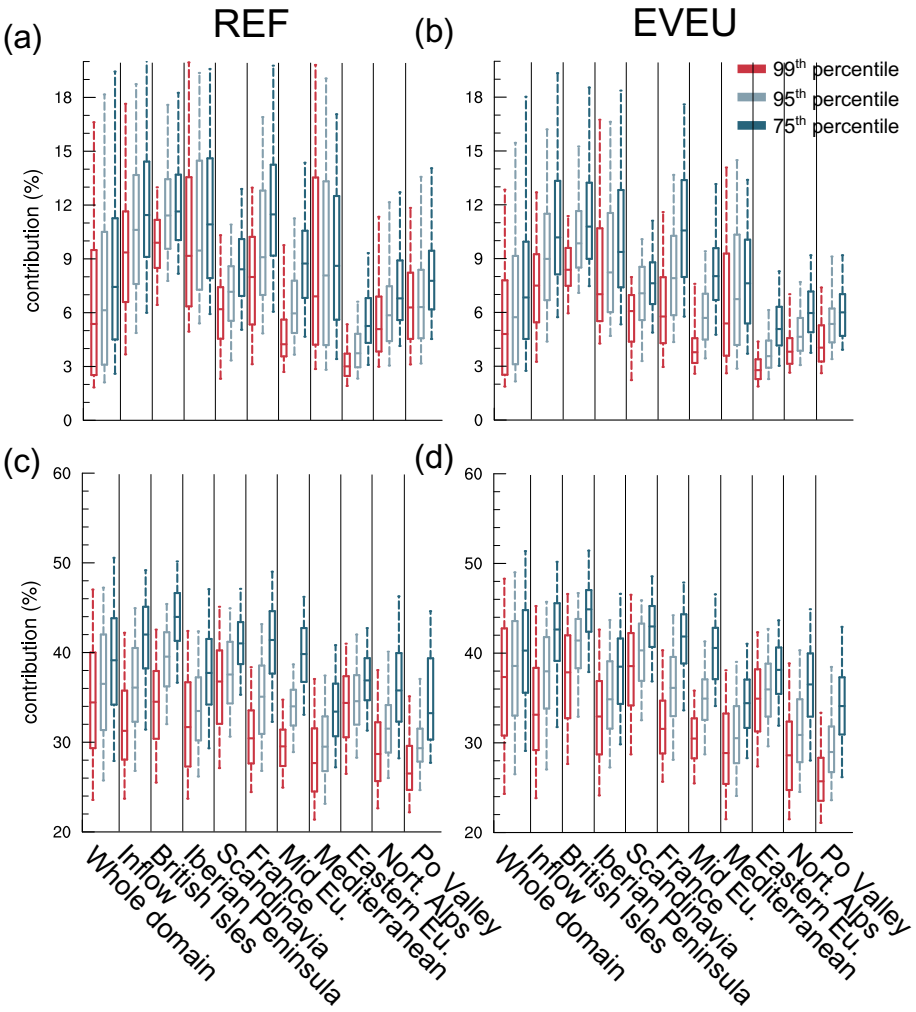

Figure S5: Box-whisker plot showing the contribution of the shipping and all other categories to ground-level ozone (in %) at the 99th, 95th and 75th percentile of ozone. **(a)** and **(b)** show the relative contributions of O_3^{shp}; **(c)** and **(d)** the relative contribution of all other sources (lightning, CH_4, stratosphere, biomass burning, and N_2O) to ozone. The lower and upper end of the box indicates the 25th and 75th percentile, the bar the median, and the whiskers the 5th and 95th percentile of the contributions of all gridboxes within the indicated region. All values are calculated for JJA of the period 2008 to 2010 and are based on 3-hourly model output. The data were transformed on a regular grid with a resolution of 0.5° x 0.5° to allow for the regional analysis.

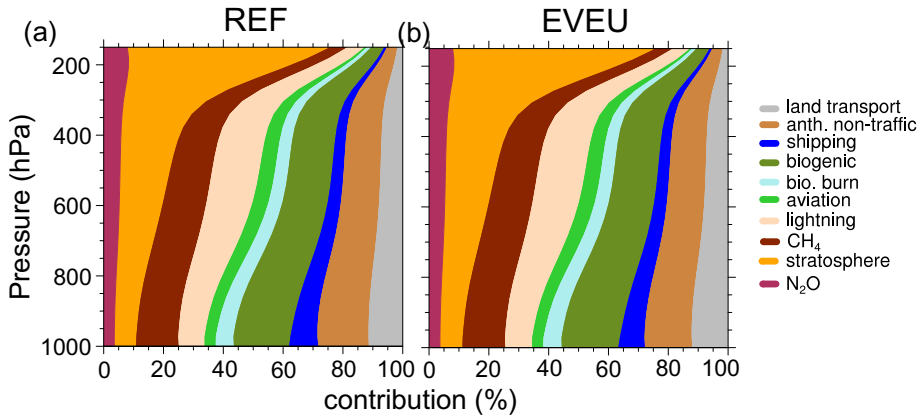

Figure S6: Vertical distribution of the area averaged (box defined as 10° W-38° E and 30° N-70° E) relative contributions of all tagged categories as simulated by **(a)** *REF* and **(b)** *EVEU*. All data are averaged for JJA 2008–2010.

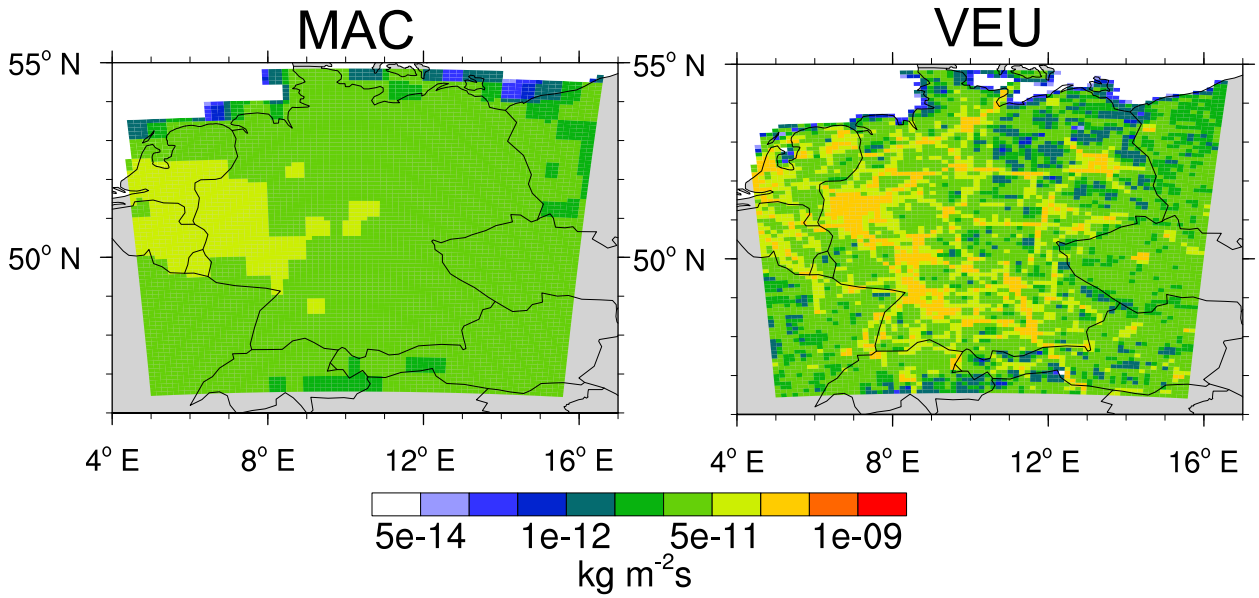

Figure S7: Comparison of NO_x emission fluxes from the land transport sector (in kg (NO) m^{-2} s^{-1}) between the MAC (left), and VEU inventories. Values are averaged for May to August 2008.

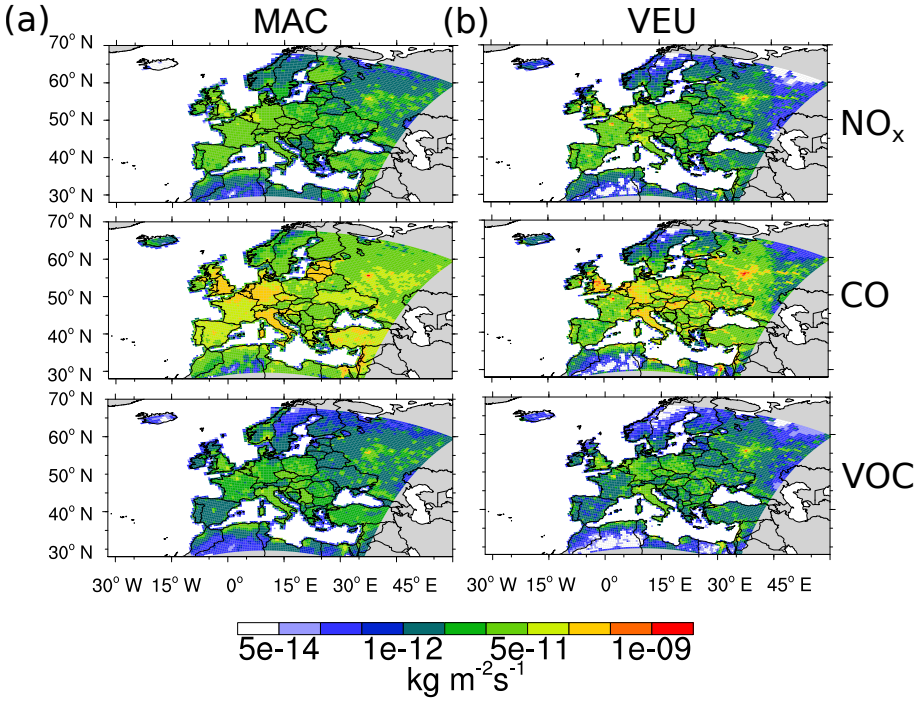

Figure S8: Annually averaged emission fluxes from the land transport sector (in kg m^{-2} s^{-1}) **(a)** MAC and **(b)** VEU emission inventories. Shown are the emissions of NO_x (in kg NO), CO (in kg CO); and VOC (in kg C).

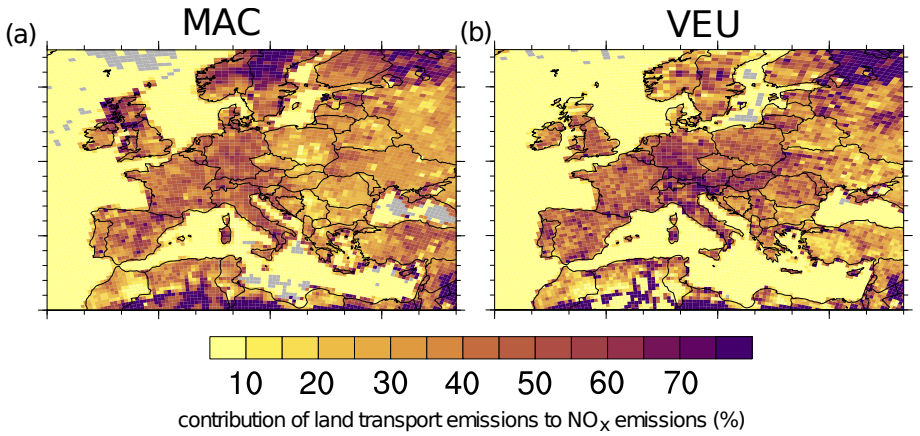

Figure S9: Relative contribution (in %) of land transport emissions to all anthropogenic emissions for July 2008. (a) shows the results for the MACCity emission inventory and (b) for the VEU emission inventory.

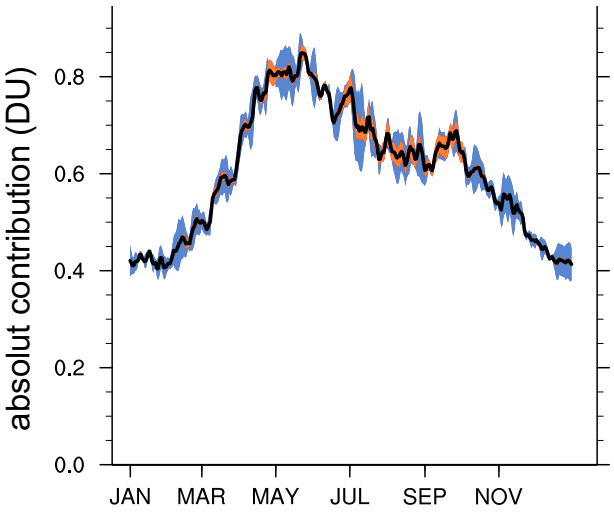

Figure S10: Seasonal cycle of the absolute contribution of land transport emissions to the ozone column up to 850 hPa (in DU).The black line indicates the mean contribution as simulated by CM50, averaged over the years 2008–2010 and the two simulations (*REF*, *EVEU*). The blue shading indicates the standard deviation with respect to time for the years 2008 to 2010 for the *EVEU* simulation. The orange shading indicates the standard deviation with respect to time between the 2008–2010 averaged seasonal cycles of the *REF* and the *EVEU* simulations.

S1 Contributions in different regions

Tables S1 - Table S2 list the absolute an relative contributions to ground-level of the different tagging categories for different geographical regions (see also Fig. 8) of the manuscript.

Table S1: Absolute (abs, in nmol mol^{-1}) and relative contributions (relative, in %) of the land transport emissions to ground-level ozone for JJA and DJF 2008–2010 in different geographical regions. Results of the *REF* simulation.

	JJA		DJF	
	relative (%)	abs. (nmol/mol)	relative (%)	abs. (nmol/mol)
Inflow	8.8	4.2	8.7	3.9
British Isles	10.2	4.4	8.8	3.4
Iberian Peninsula	11.0	6.0	8.9	3.9
France	11.2	5.2	8.9	3.2
Mid Europe	13.1	5.8	8.8	2.6
Scandinavia	11.1	4.8	8.7	3.1
Northern Alps	13.7	7.0	9.0	6.7
Mediterranean	12.8	7.4	9.9	4.5
Eastern Europe	12.1	5.6	9.2	3.3
Po Valley	14.0	7.5	9.5	3.5

Table S2: Absolute (abs, in nmol mol^{-1}) and relative contributions (relative, in %) of the land transport emissions to ground-level ozone for JJA and DJF 2008–2010 in different geographical regions. Results of the *EVEU* simulation.

	JJA		DJF	
	relative (%)	abs. (nmol/mol)	relative (%)	abs. (nmol/mol)
Inflow	9.1	4.2	8.7	4
British Isles	10.0	4.1	8.8	3.4
Iberian Peninsula	12.1	6.4	9.2	3.9
France	12.1	5.4	9.2	3.2
Mid Europe	14.3	5.9	9.1	2.7
Scandinavia	10.9	4.6	8.8	3.2
Northern Alps	15.8	7.7	9.3	3.7
Mediterranean	14.4	8.1	10.2	4.6
Eastern Europe	13.5	6.0	9.6	3.3
Po Valley	16.2	8.0	9.9	3.2

Table S3: Absolute (abs, in nmol mol^{-1}) and relative contributions (relative, in %) of anthropogenic emissions (anthropogenic non-traffic, shipping and aviation) to ground-level ozone for JJA and DJF 2008–2010 in different geographical regions. Results of the *REF* simulation.

	JJA		DJF	
	relative (%)	abs. (nmol/mol)	relative (%)	abs. (nmol/mol)
Inflow	33.9	15.7	33.3	15.4
British Isles	32.5	13.9	32.9	12.8
Iberian Peninsula	32.3	17.8	33.6	14.8
France	32.6	15	33.4	11.9
Mid Europe	31.7	14	32.8	9.9
Scandinavia	30.5	13.3	32.1	11.4
Northern Alps	30.7	15.5	33	13.6
Mediterranean	32.6	18.9	35.7	16.4
Eastern Europe	29.9	13.8	33.4	11.8
Po Valley	31.0	16.6	34.3	12.6

Table S4: Absolute (abs, in nmol mol^{-1}) and relative contributions (relative, in %) of anthropogenic emissions (anthropogenic non-traffic, shipping and aviation) to ground-level ozone for JJA and DJF 2008–2010 in different geographical regions. Results of the *EVEU* simulation.

	JJA		DJF	
	relative (%)	abs. (nmol/mol)	relative (%)	abs. (nmol/mol)
Inflow	33.2	15.1	33.2	15.3
British Isles	31.6	12.9	32.8	12.8
Iberian Peninsula	30.3	16.0	33.1	14.2
France	30.5	13.5	33.0	11.7
Mid Europe	28.9	11.8	32.3	9.5
Scandinavia	29.6	12.5	31.8	11.6
Northern Alps	27.6	13.3	32.4	12.8
Mediterranean	29.6	16.7	34.7	15.6
Eastern Europe	27.0	11.9	32.6	11.3
Po Valley	28.1	13.8	33.5	11.0

Table S5: Absolute (abs, in nmol mol^{-1}) and relative contributions (relative, in %) of all other categories (categories CH_4, N_2O, lightning, stratosphere, and biomass burning) to ground-level ozone for JJA and DJF 2008–2010 in different geographical regions. Results of the *REF* simulation.

	JJA		DJF	
	relative (%)	abs. (nmol/mol)	relative (%)	abs. (nmol/mol)
Inflow	42.9	19.3	46.8	21.51
British Isles	42.0	17.4	47.12	18.27
Iberian Peninsula	37.9	20.7	46.2	20.14
France	38.4	17.7	46.6	16.5
Mid Europe	36.3	15.9	47.4	14.4
Scandinavia	42.7	18.1	48.1	17.2
Northern Alps	36.9	19.5	47.1	19.2
Mediterranean	35.3	20.5	43.5	19.8
Eastern Europe	38.6	17.8	46.5	16.5
Po Valley	36.1	19.2	45.3	16.6

Table S6: Absolute (abs, in nmol mol^{-1}) and relative contributions (relative, in %) of all other categories (categories CH_4, N_2O, lightning, stratosphere, and biomass burning) to ground-level ozone for JJA and DJF 2008–2010 in different geographical regions. Results of the *EVEU* simulation.

	JJA		DJF	
	relative (%)	abs. (nmol/mol)	relative (%)	abs. (nmol/mol)
Inflow	43.3	19.2	46.9	21.6
British Isles	42.7	17.2	47.2	18.4
Iberian Peninsula	38.5	20.2	46.5	19.9
France	39.1	17.5	46.8	16.6
Mid Europe	37.4	15.1	47.6	14.1
Scandinavia	43.5	17.9	48.2	17.7
Northern Alps	37.4	18	47.4	18.6
Mediterranean	36.1	20.3	44.1	19.7
Eastern Europe	39.6	17.5	46.9	16.4
Po Valley	36.5	17.9	45.6	15.0

Table S7: Absolute (abs, in nmol mol^{-1}) and relative contributions (relative, in %) of the biogenic category to ground-level ozone for JJA and DJF 2008–2010 in different geographical regions. Results of the *REF* simulation.

	JJA		DJF	
	relative (%)	abs. (nmol/mol)	relative (%)	abs. (nmol/mol)
Inflow	14.4	6.6	11.2	5.0
British Isles	15.2	6.3	11.2	4.2
Iberian Peninsula	18.8	10.5	11.2	4.9
France	17.8	8.4	11	3.8
Mid Europe	18.8	8.3	11	3.3
Scandinavia	15.7	6.6	11.1	3.9
Northern Alps	18.8	9.6	10.9	4.4
Mediterranean	19.3	11.3	10.9	5
Eastern Europe	19.3	9	10.9	3.8
Po Valley	19.0	10.2	10.9	4.0

Table S8: Absolute (abs, in nmol/mol^{-1}) and relative contributions (relative, in %) of the biogenic category to ground-level ozone for JJA and DJF 2008–2010 in different geographical regions. Results of the *EVEU* simulation.

	JJA		DJF	
	relative (%)	abs. (nmol/mol)	relative (%)	abs. (nmol/mol)
Inflow	14.5	6.5	11.2	5
British Isles	15.6	6.3	11.2	4.3
Iberian Peninsula	19.1	10.2	11.3	4.8
France	18.3	8.3	11	3.8
Mid Europe	19.5	8	11	3.2
Scandinavia	16	6.5	11.1	4
Northern Alps	19.2	9.4	10.9	4.2
Mediterranean	19.9	11.3	11	4.9
Eastern Europe	19.9	8.9	10.9	3.8
Po Valley	19.3	9.6	10.9	3.6

S2 Model evaluation

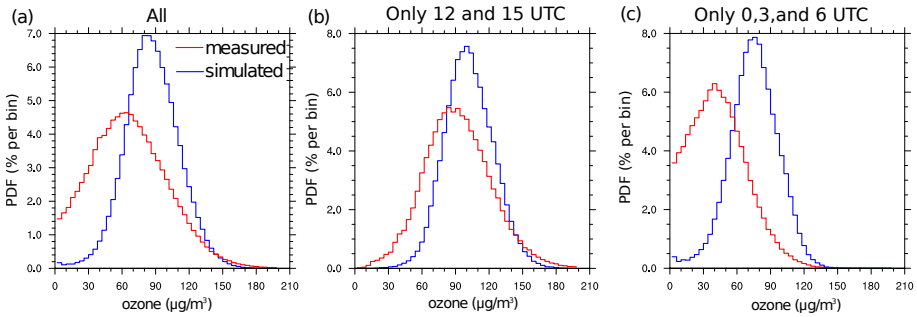

Figure S11: Probability density functions (PDFs) of observed and simulated ozone concentrations (in μgm^{-3}) at all considered Airbase stations. The observations were subsampled on the model output frequency (every 3 hours). (a) shows the PDF considering all values (based on model output every 3 hours. (b) shows the PDF considering only observations/model results at 12 and 15 UTC. (c) shows the PDF considering only observations/model results at 0, 3 and 6 UTC. Results of the *REF* simulation.

S3 Definition of the regional subdomains

The definition of the ten geographical regions is given in Fig. S12. The names of the different regions is listed in Table S9. The definition is largely based on the definition of the PRUDENCE regions (Christensen et al., 2007), but we decompose their region 'Alps' into 'Po Valley' and 'Northern Alps'. In addition a region 'Inflow' is defined.

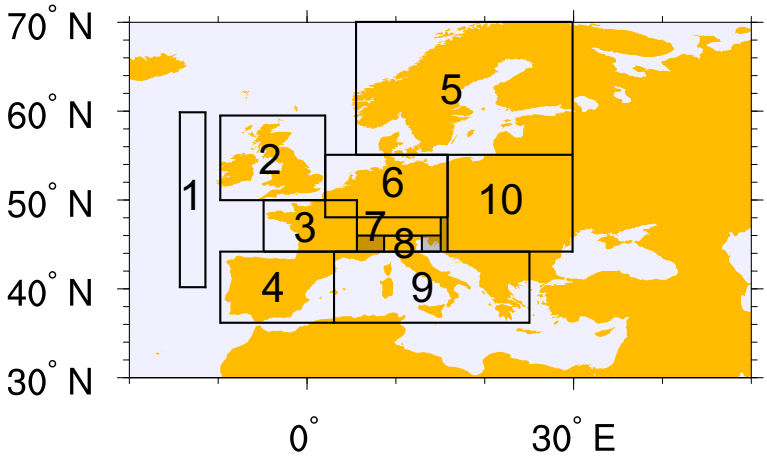

Figure S12: Geographical definition of the ten subdomains (black, 1–10) used for analyses. The three small regions around the Alps which are greyed out are not analysed. The corresponding names are listed in Table S9.

Table S9: Name of the different geographical regions. The first row (Nr.) indicates the number of the domain as in Fig. S12.

Nr.	Name
1	Inflow
2	British Isles
3	France
4	Iberian Peninsula
5	Scandinavia
6	Mid Europe
7	Northern Alps
8	Po Valley
9	Mediterranean
10	Eastern Europe

S4 Emission totals

The following Tables summaries the emissions of NO_x, CO and VOCs from all anthropogenic and natural sources applied in the different simulations. Please note, that for every specie only these emission sectors are given where emissions occur. These sectors are:

- **road t.**: land transport emissions
- **anth. nt**: Anthropogenic non-traffic emissions
- **shipping**: Shipping emissions
- **aviation**: Aviation emissions
- **Soil-**NO_x: NO_x emissions from soils calculated by the model
- **LNOX**: Lightning NO_x emissions
- **AWB**: Agricultural waste burning emissions
- **BB** : Biomass burning emissions
- **biog.**: Further biogenic emissions, not calculated by the model but prescribed as annual climatology
- **biog.** C_5H_8: Biogenic isoprene emissions, calculated by the model

Tables S10–S12 list the total emissions of EMAC for NO_x, CO and VOC, respectively. Please note, that the given total emissions for C_5H_8 from biogenic origin are scaled with 0.6 for EMAC (Jöckel et al., 2006) and 0.45 for COSMO/MESSy (Mertens et al., 2016).

Table S10: Total emissions of NO_x (in Tg a^{-1} in amount of NO) for EMAC. Given are the annual totals averaged the years 2008 to 2010.

Simulation	road t.	anth. nt	shipping	aviation	Soil NO_x	LNOX	AWB	BB	Sum
REF	20.4	37.0	12.8	2.2	12.7	12.4	0.418	10.7	109
EVEU	20.4	37.0	12.8	2.2	12.7	12.4	0.418	10.7	109

Table S11: Total emissions of CO (in (in Tg a^{-1}) for EMAC. Given are the annual totals averaged the years 2008 to 2010.

Simulation	road t.	anth. nt	shipping	AWB	biog.	BB	Sum
REF	149	415	1.34	20.3	113	406	1100
EVEU	149	415	1.34	20.3	113	406	1100

Table S12: Total emissions of VOC (in Tg a^{-1} in amount of C) for EMAC. Given are the annual totals averaged the years 2008 to 2010.

Simulation	road t.	anth. nt	shipping	biog. C_5H_8	AWB	biog.	BB	Sum
REF	17.4	73.4	2.30	282	0.943	108	14.5	498
EVEU	17.4	73.4	2.30	282	0.943	108	14.5	498

Table S13: Total emissions of NO_x (in Tg in amount of NO) for CM12. Given are the annual totals for the May to August 2008.

Simulation	road t.	anth. nt	shipping	aviation	Soil NO_x	LNOX	AWB	BB	Sum
REF	0.342	0.335	0.0333	0.0642	0.167	0.0456	0.000761	0.00361	0.988
EVEU	0.441	0.277	0.0263	0.0555	0.167	0.0456	0.000761	0.00361	1.01

Table S14: Total emissions of CO (in Tg) for CM12. Given are the annual totals for the May to August 2008.

Simulation	road t.	anth. nt	shipping	AWB	biog.	BB	Sum
REF	1.27	1.41	0.00348	0.0333	4.81	0.12	7.65
EVEU	1.18	0.842	0.000719	0.0333	4.81	0.12	6.98

Table S15: Total emissions of VOC (in Tg in amount of C) for CM12. Given are the annual totals for the May to August 2008.

Simulation	road t.	anth. nt	shipping	biog. C_5H_8	AWB	biog.	BB	Sum
REF	0.141	0.538	0.00413	0.423	0.0111	0.372	0.00516	1.49
EVEU	0.143	0.383	0.00175	0.423	0.0111	0.372	0.00516	1.34

S5 Ozone production and loss terms

The diagnosed production (ProdO3) and loss rates (LossO3) of ozone as analysed in the manuscript follow the definition of production and loss of the odd oxygen family as used in the TAGGING submodel (see Grewe et al., 2017). Compared to other definitions of production and loss rates of tropospheric ozone our definition takes also the production of ozone by photolysis of oxygen into account. For diagnosing the production and loss rates the TAGGING submodel uses diagnostic tracers in MECCA (Sander et al., 2011). Table S16 lists the names of the four diagnostic ozone production and the five diagnostic ozone loss tracers. The summed tendencies from all 'o3prod*' tracers are defined as ProdO3 and the sum of the tendencies from all 'o3loss' tracers are defined as LossO3. Please note, that the tendency from the tracer o3prodo2 is multiplied with a factor of two, as the reaction leads to two O^1D molecules. All reactions which are considered as source/loss of odd oxygen are marked with the name of the respective diagnostic tracer on the right hand side in Tables showing the chemical mechanism (which is also part of the Supplement).

Table S16: Names of the diagnostic ozone production/and loss tracers.

Prodo3	LossO3
o3prodro2	o3lossho2
o3prodho2	o3lossoh
o3prodo2	o3lossro
ProdMeO2	o3lossno
	o3lossxo

S6 References

References

Christensen, J. H., Carter, T. R., Rummukainen, M., and Amanatidis, G.: Evaluating the performance and utility of regional climate models: the PRUDENCE project, Climatic Change, 81, 1–6, doi:10.1007/s10584-006-9211-6, URL http://dx.doi.org/10.1007/s10584-006-9211-6, 2007.

Grewe, V., Tsati, E., Mertens, M., Frömming, C., and Jöckel, P.: Contribution of emissions to concentrations: the TAGGING 1.0 submodel based on the Modular Earth Submodel System (MESSy 2.52), Geosci. Model Dev., 10, 2615–2633, doi:10.5194/gmd-10-2615-2017, URL https://www.geosci-model-dev.net/10/2615/2017/, 2017.

Jöckel, P., Tost, H., Pozzer, A., Brühl, C., Buchholz, J., Ganzeveld, L., Hoor, P., Kerkweg, A., Lawrence, M., Sander, R., Steil, B., Stiller, G., Tanarhte, M., Taraborrelli, D., van Aardenne, J., and Lelieveld, J.: The atmospheric chemistry general circulation model ECHAM5/MESSy1: consistent simulation of ozone from the surface to the mesosphere, Atmos. Chem. Phys., 6, 5067–5104, doi:10.5194/acp-6-5067-2006, URL http://www.atmos-chem-phys.net/6/5067/2006/, 2006.

Mertens, M., Kerkweg, A., Jöckel, P., Tost, H., and Hofmann, C.: The 1-way on-line coupled model system MECO(n) – Part 4: Chemical evaluation (based on MESSy v2.52), Geosci. Model Dev., 9, 3545–3567, doi:10.5194/gmd-9-3545-2016, URL http://www.geosci-model-dev.net/9/3545/2016/, 2016.

Mertens, M. B.: Contribution of road traffic emissions to tropospheric ozone in Europe and Germany, URL http://nbn-resolving.de/urn:nbn:de:bvb:19-207288, 2017.

Sander, R., Baumgaertner, A., Gromov, S., Harder, H., Jöckel, P., Kerkweg, A., Kubistin, D., Regelin, E., Riede, H., Sandu, A., Taraborrelli, D., Tost, H., and Xie, Z.-Q.: The atmospheric chemistry box model CAABA/MECCA-3.0, Geosci. Model Dev., 4, 373–380, doi:10.5194/gmd-4-373-2011, URL http://www.geosci-model-dev.net/4/373/2011/, 2011.